Egypt.J.Chem. **Vol. 62**, Special Issue (Part 2), pp. 797-817 (2019)

Egyptian Journal of Chemistry
http://ejchem.journals.ekb.eg/

Synthesis of Zinc Oxide and Silver/ Zinc Oxide Nanocomposite for Production of Antimicrobial Textiles

I. Othman Ali[1, 2], M.M. El-Molla[1, 3*]

[1]*Chemistry Department, College of Sciences & Art, - Gurayyat. Jouf University, Saudi Arabia*

[2]*Department of Chemistry, Faculty of Science, Al-Azhar University, Nasr City, 11884, Cairo, Egypt*

[3]*Textile Research Division, National Research Centre El- Bohouth St., Dokki, Giza, P.O.12622, Egypt*

THE zinc oxide nanoparticles were prepared by using Co-precipitation method and synthesis of Ag nanoparticles embedded in zinc oxide based on the reaction of silver nitrate with zinc oxide in one-step, after that these compounds were directly applied on to the 100% cotton woven fabric using a printing paste containing these compounds. These compounds are fixed onto cotton fabrics by dry with a low temperature and then thermo fixed method. The synthetized zinc oxide and / or silver/ zinc oxide were studied to prove its structure using various analyses such as X-ray, AFM analyses, IR spectra, the scanning electron microscopy (SEM) ….etc. Blends mixing calculation indicted the distribution of ZnO through CMC more favorable than Ag. Molecular dynamic simulation demonstrated that H-bond and electrostatic effect between nanoparticle and CMC should be the main driving forces to make nanoparticle molecules be adsorbed on the CMC and have slow-release properties in water or in water environment. Moreover, the antibacterial activity of printed cotton fabrics with, either synthetized zinc oxide and / or silver/ zinc oxide against, Staphylococcus aureus and Escherichia coli was evaluated. Docking study was carried out to indicate interaction behavior of sample with DNA grays of microorganism. Docking study showed that, the hydrophilicity of the sample due to presence nanoparticles, which was the circular key for inhibiting microorganism. The novelty of this work was arisen from its ability to fit the requirements of economic feasibility of medical textile.

Keywords: Nanoparticles, Zinc oxide, Cotton fabrics, Silver zinc oxide, Antimicrobial textiles, Docking simulation.

Introduction

The application of nanoscale materials and structures, usually ranging from one to 100 nanometers (nm), is an emerging area of nanoscience and nanotechnology. Synthesis of noble metal nanoparticles for applications such as catalysis, electronics, textiles, environmental protection, and biotechnology is an area of constant interest. Recently, an awareness of general sanitation, contact disease transmission, and personal protection has led to the development of antimicrobial textiles [1].

Cellulosic textiles can now be durably functionalized to make them antimicrobial, UV-protective, Self-cleaning, flame retardant, stain/ water repellent, air-permeable, hydrophobic, electrically conductive, photo-luminescent and pollutant removing, while retaining comfort. These traits can be achieved by new methodologies with various functionalizing agents based on metal salts. Metal oxides, metal nanoparticles, and metal–organic [2].

Textile fabric provides an excellent environment for the growth of microorganisms because of their large surface area and the ability to retain moisture. Increasing microbial resistance have emerged as a major challenge to the healthcare systems and despite the wide range

*Corresponding author e-mail:: mmelmolla@ju.edu.sa, mohamedelmolla212@gmail.com
Received 01/10/2019; Accepted 17/11/2019
DOI: 10.21608/ejchem.2019.17392.2083

of the available antimicrobial therapies, microbial infections remain high, due to the ability of these organisms to develop resistance to virtually all antimicrobial therapies. A large number of chemicals have been used to impart antimicrobial activity to textile materials. More attention has been paid on the preparation and applications of nano-metal oxide coatings onto cotton substrate due to their promising applications [3, 4].

Nowadays, metal oxides nanoparticles coated onto cotton fibers represent important composites that are increasingly being developed for use in novel health-related applications [5-7]. Inorganic additives combine biocidal and biostatic properties, therefore, the use of inorganic compounded into the polymer matrix, the so-called antimicrobial polymer systems, can produce a good antibacterial effect for medical application [8]. Combinations of different metals, metal oxides and particle coatings were investigated and found as even more promising [9, 10].

Silver NP-impregnated products such as wound dressings, textile fabrics, and catheters have rapidly conquered the market [11]. As conducting polymers alone are known to have antibacterial properties [12], their combination with silver may result in synergistic action and enhanced antimicrobial performance [13, 14]. The composites of conducting polymers with silver [15] can be produced in single step by the oxidation of respective monomers with silver salts [16, 17]. Alternatively, both polyaniline [14, 18] and poly pyrrole [19], are known to reduce silver compounds to corresponding metal, and this approach has been used in the present communication. Tiam et al [20] found that Ag nanoparticles not only have antibacterial activity, but also have wound healing properties. It can restore burnt skin to the normal skin. Yet, other inorganic NP have shown antibiotic properties such as gold [21], copper [22], copper oxide [23] titanium dioxide [24] and zinc oxide [25].

Zinc oxide is of particular interest due to their comparably modest cost and their established use in health care products [26]. Recently, several studies have demonstrated quite efficient antimicrobial activity of zinc Oxide nano particles against gram-positive and gram-negative bacteria [27, 28]. Several attempts to design various silver/zinc oxide nanocomposites with an antibacterial activity against gram positive and gram-negative bacteria have been introduced in the literature [29, 30]. K. Rana et al. [31] use poly (allyl amine) for the formation and coating of silver/zinc oxide from a simple water-soluble zinc salt under mild conditions for developing self-cleaning flexible materials.

The present work was carried out with the following objectives, synthetized zinc oxide and / or silver / zinc oxide nanoparticles and it is utilize for printed cotton fabrics, in order to get on anti-bacteria of textile cotton fabrics i.e. (medical textiles)

Experimental

Materials

Cotton fabric

Mill scoured fabric and bleached cotton fabric160g/m^2, (kindly supplied by Miser Co., El-Mahalla Elcobra. Egypt) was treated with a solution of 5g/l sodium carbonate (Merck, Germany) and 2g/l nonionic detergent (Host pal C.V. from Clariant) at 95°Cfor 1/2 hour, thoroughly rinsed and air-dried at room temperature.

Chemicals

Silver nitrate, zinc acetate and sodium hydroxide (Merck, Germany). Carboxy methyl Cellulose (CMC) molecules (SD Fine chem. Limited, high viscosity 98%, India). All the chemicals were analytical grade reagents and employed as received without having more filtration.

Methods

Synthesis of Zinc Oxide nanoparticles by Co-precipitation method

Fine particles of zinc oxide nanoparticles were prepared by using Co-precipitation method [32]. Stoichiometric amount of Zn $(AC)_2$ (2.15g), CMC (1.0 g) were continuously dissolved in distilled water and mixed with vigorous stirring; after that, the mixture was heated up to 85 ºC for 30 min. At this stage, (Na OH) solution was added drop by drop to the mixture until solution pH (7.8) attained suitable condition for co-precipitation of the cation from the solution to synthesize nanoparticles. In this study, the preferred solution pH was 7.8 when a white precipitate was formed, the addition of (Na OH) was stopped and the solution was stirred for 2 h at 80 °C to ensure complete crystallization and growth of the nanoparticles. Then the stirrer was turned off and the precipitates were filtered and the mother liquor was checked for complete precipitation by adding few drops of Na OH solution. Then the precipitate was dried at 120°C for 4 h. The powder was finally claimed at 450° C for 6 h; the sample was referred as zinc oxide.

Fabrication of Silver-decorated zinc oxide nanoparticles

One-step synthesis of Silver nanoparticles embedded in zinc oxide based on the reaction of silver nitrate with zinc oxide was applied [33]. No other additive was considered either to promote the reaction or to protect growth of Silver seeds. In a typical procedure, a stock solution of 0.1M $AgNO_3$ was prepared and kept in the dark for protection against light impact. To prepare the silver / zinc oxide NPs sample, 15 ml $AgNO_3$ solution was added drop by drop to an aqueous Zinc Oxide suspension (2g/100 ml) at pH = 7.0 in a quartz cell (22 mm diameter and 245 mm height) with constant stirring at 50 ºC. The resulting mixture was then subjected to UV-irradiation using a high-pressure mercury lamp (365 nm and 8W) for 15 min under continuous stirring and flowing nitrogen atmosphere at room temperature. UV exposure resulted into reduction of Ag^+ ions to Ag nanoparticles, which was corroborated by change in color from white to moss green. After the reaction has finished, an appropriate cut off filter was placed in the front of the reactor to remove the portion of the UV irradiation. Finally, the solid product so obtained was filtered and washed with distilled water then dried in oven at 80 ºC; the sample was referred as silver/ zinc oxide.

Application onto cotton fabrics

Synthetized of zinc oxide and silver / zinc oxide nano composite were applied on cotton fabrics using the printing paste. The printing pastes for printing cotton fabrics were prepared according to the following recipe:

Carboxy Methyl Cellulose	40 g
Synthetized of zinc oxide and / or silver / zinc oxide *	X g
Acrylic binder	10 g
Water	Y g
Total	1000 g

*The synthetized of zinc oxide and / or silver / zinc oxide used was either 1, 2, or 3%

Printing technique

The pastes were applied to the fabric through screen printing process. After printing and drying the fabric was cured for 3 min at 140°C, using an automatic thermo static oven (Wemer Mathis Co., Switzer land). The fabric was then immersed for 5 min in 2 g/l of sodium lauryl sulfate to remove unbound nanoparticles. Then the fabric was rinsed to completely take out all the soap solution. The fabric thus washed was air-dried.

Measurements and Analysis

X-ray diffraction analysis

Phase identification, purity, relative crystallinity and crystallite size of the products were performed at room temperature by using a Philips diffractometer (type PW 3710). The patterns were run with Ni-filtered copper radiation ($\lambda = 1.5404$ Å) at 30 kV and 10 mA with a scanning speed of 2θ =2.5º/min.

Infrared analysis

The infra-red of the synthetized of zinc oxide and silver / zinc oxide nanocomposite were measured using Infra-red spectrometer, Perkin Elmer, system 2000 FT-IR (Fourier transform IR spectrometer). Single beam spectrometer with a resolution of 2 cm^{-1}. The samples were ground with KBr (1:100 ratio) as a tablet and mounted to the sample holder in the cavity of the spectrometer.

Diffuse Reflectance Ultraviolet–visible spectroscopy

Diffuse Reflectance Ultraviolet–visible spectroscopy (UV–vis DRS) of the samples was carried out at room temperature using UV–vis JASCO spectrophotometer, V-570, in the range of 200–1000 nm.

Scanning Electron Microscope (SEM)

Synthetized of zinc oxide and silver / zinc oxide nanocomposite and / or finishing fabrics of cotton with synthetized of zinc oxide and silver / zinc oxide nanocomposite are mounted on aluminum stubs, and sputter coated with gold in a 150 Å sputter (Coated Edwards), and examined by Jeol (JXA-840A) Electron Probe Microanalysis (Japan), magnification range 35-10,000, accelerating voltage 19 kV. In order to confirm the presence of fragrance particles.

Atomic Force Microscopy (AFM)

The surface topological study was carried out by atomic force microscopy (AFM) using Wet-SPM9600 (Scanning Probe microscope) Shimadzu made in Japan.

Antibacterial activity testing

Antimicrobial activity of the tested treated fabrics against Gram-positive bacteria (Staphylococcus aureus, SA) and Gram-negative bacteria (Escherichia coli, EC) was tested according to AATCC Test Method 100-1999**.**

Computational study

Preparation of small molecule

The target compounds were built using and minimized their energy with PM3 through MOPAC then DFT using B3LYP/6-311G. All the Quantum

chemical computations were performed, using the PM3 semi-empirical Hamiltonian molecular orbital calculation MOPAC16 package, then employing density function theory in Gaussian 09 W program package with the Becke3-Lee-Yang-parr (B3LYP) level using 6-311G* basis as implemented in Molecular Operating Environment 2015 package Molecular Operating Environment. The optimization Geometry for molecular structures were carried out, for improve knowledge of chemical structures. Our compounds were introduced into the binding sites according to the published crystal structures.

Selection of proteins structures

Docking experiment was carried out for the target active site into DNA Gyrase B (ID: 4uro) using Molecular Operating Environment 2015. The structure preparation process in Molecular Operating Environment corrected the errors of active sites. After the correction, hydrogens were added and partial charges (Gasteiger methodology) were calculated. Energy minimization (AMBER12: EHT, root mean square gradient: 0.100) was performed.

Molecular dynamics simulations

A model composed of CMC molecule and one ZnO molecule was selected from the blending calculation results. NPT MD simulations were carried out in 15 ns at 300 K for the selected model. In the NPT MD simulations, the first 5 ns was used for equilibration, and the next 10 ns was used to collect data. CMC/ZnO model is in a water box containing 500 water molecules was constructed by using Amorphous Cell software. Water box (100 x 100 x 120 Å) which neutralized with Na Cl. The periodic boundary conditions for this box have been applied at constant volume and pressure with 10 Å cutoff for nonbonding interactions. After a steepest-descent energy minimization (AMBER12: EHT), the system was heated from zero to 310 K with 100 ps, then by 50 ps for equilibration simulation before each MD simulation (position restraints on all protein and ligand heavy atoms). Finally, the system was simulated for 1 ns at constant temperature (300 K, Langevin, default values) and pressure (1 bar, Nose-Hoover Langevin, default values), without any position restrains. The time step was set to 0.002 fs and all bonds were constrained.

Binding site analysis

The binding site of each receptors were identified through the Molecular Operating Environment Site Finder program, which uses a geometric approach to calculate putative binding sites in a protein, starting from its tridimensional structure. This method is not based on energy models, but only on alpha spheres, which are a generalization of convex hulls. The prediction of the binding site performed by the Molecular Operating Environment Site Finder module, confirmed the binding sites defined by the co-crystallized ligands in the holo-forms of the investigated proteins.

Molecular Operating Environment Stepwise Docking Method

The crystal structure of the active site complexed with reference inhibitor was obtained. Water and inhibitor molecule were removed, and hydrogen atoms were added. The parameters and charges were assigned with MMFF94x force field. After alpha-site, spheres were generated using the site finder module of Molecular Operating Environment. The optimized 3D structures of molecules were subjected to generate different poses of ligands using triangular matcher placement method, which generating poses by aligning ligand triplets of atoms on triplets of alpha spheres represented in the receptor site points, a random triplet of alpha sphere center was used to determine the pose during each iteration. The pose generated was rescored using London dG. Scoring function. The poses generated refined with MMFF94x force field, also, the solvation effects were treated. The Born solvation model (GB/VI) was used to calculate the final energy, and the finally assigned poses were assigned a score based on the free energy in kcal/mol.

Result and Discussion

X-ray powder diffraction

Figure 1 shows the XRD patterns for zinc oxide nanoparticles and silver / zinc oxide nanocomposites. All samples showed strong and sharp diffraction peaks at 2θ = 31.8°, 34.4º, 36.2º, 47.5º, 56.6º, 62.8º, 66.4º, 67.9º and 69.1º corresponding to the diffraction planes (100), (002), (101), (102), (110), (103), (200), (112) and (201) planes, respectively. The reflections at 2θ = 31.8º, 34.4º and 36.2º confirmed the presence of hexagonal Zinc Oxide phase with a quartzite structure with space group (P63mc) for all samples. The diffraction data also showed good agreement with the JCPDS card for zinc oxide (JCPDS Card No. 36-1451) [34].

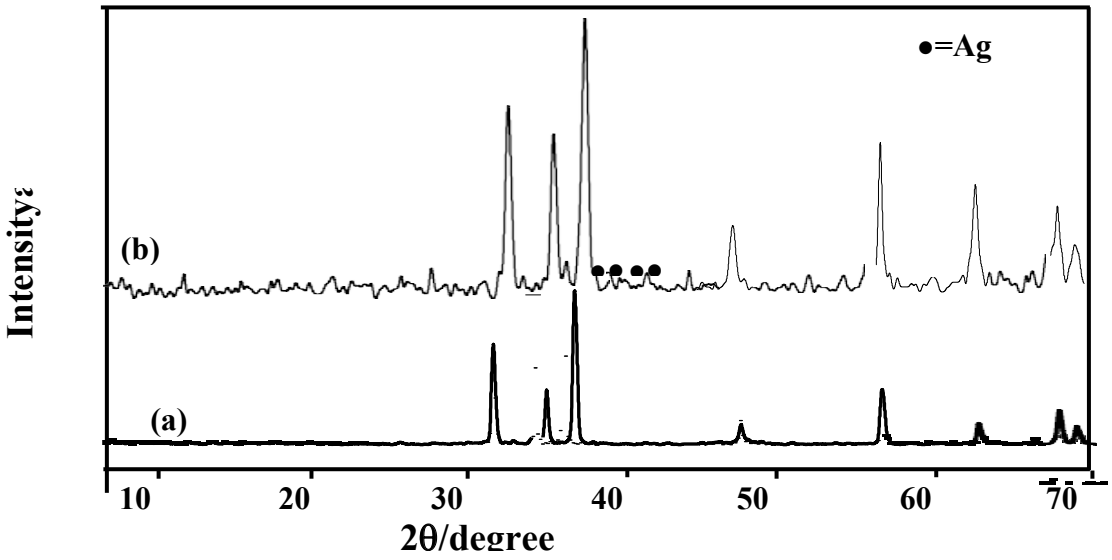

Fig. 1. The XRD patterns for synthetized zinc oxide nanoparticles and silver / zinc oxide nanocomposites.

The obtained patterns indicate that the synthesized samples are crystalline single phase without impurities.

Meanwhile, the XRD pattern of silver / zinc oxide nanoparticles showed two small peaks at 37.9º and 44.2º corresponding to (111) and (2 0 0) crystal planes of metallic Ag, respectively, confirming the presence of Ag in the sample. No shift in the peak positions of zinc oxide indicating that silver particles are positioned on the surface of zinc oxide nanoparticles, thereby one can exclude the possibility of silver particle either going into the lattice of zinc oxide or substituting zinc site [35]. It must be mentioned that other silver diffraction peaks were not observed in the XRD patterns of silver / zinc oxide nanoparticles. This is probably due to the small quantity of Silver nanoparticles and/or excellent dispersion on the zinc oxide. The strong intensity of peaks in the pattern of the silver / zinc oxide sample compared with those of zinc oxide synthesized with different methods confirms that the nanostructured Silver/ zinc oxide were based on the zinc oxide with the preferential orientation growth along c- axis of zinc oxide nanostructures.

FT-IR spectra

Figure 2 shows the FT-IR spectra of zinc oxide and silver / zinc oxide in the range from 4000-400 cm^{-1}. The FT-IR spectra of zinc oxide showed a broad band at 3431 cm^{-1}which corresponds to the O-H stretching vibration. The observed bands at 2973 and 2865$cm^{-1}$are assigned to the anti-symmetric and symmetric of CH_2-vibrations, respectively of the carbon chains in the CMC structure. Zinc oxide spectra showed a band at 506 cm^{-1}assigned to the characteristic stretching mode of Zn-O bond [36-38].

The absorption band at 880 $cm^{-1}$of zinc oxide is due to the formation of tetrahedral coordination of Zn-O, and the bands at 1439 and 1043 cm^{-1}related to stretching modes of C-O and C=O, respectively.

FT-IR spectra of silver / zinc oxide shown a decrease the OH band at 3431 cm^{-1}in the spectrum of zinc oxide with lower shift to 3418 $cm^{-1}$when compared with the comparable band in the spectrum of silver / zinc oxide.This observation to be concurrent with a decrease in the relative band intensity at 472 cm^{-1}assigned to Zn-O stretch in the spectrum of silver / zinc oxide, showing that -OH on the zinc oxide is involved in the process of formation of silver nanoparticles.

UV-visible absorption study

As shown in Fig. 3 the UV-vis absorption spectra of zinc oxide and silver / zinc oxide nanocomposites material were recorded at room temperature. The spectra reveal a characteristic absorption band of silver / zinc oxide nanocomposite material at 363 nm [39, 40]. The absorbance increases in the higher wavelength side indicating the role of nano silver particles in zinc oxide.

A great number of silver is dispersed into zinc oxide and these metallic particles rest on the surface of zinc oxide nanocomposite making the surface area more and showing plasmonic resonance band in the UV-vis spectra.

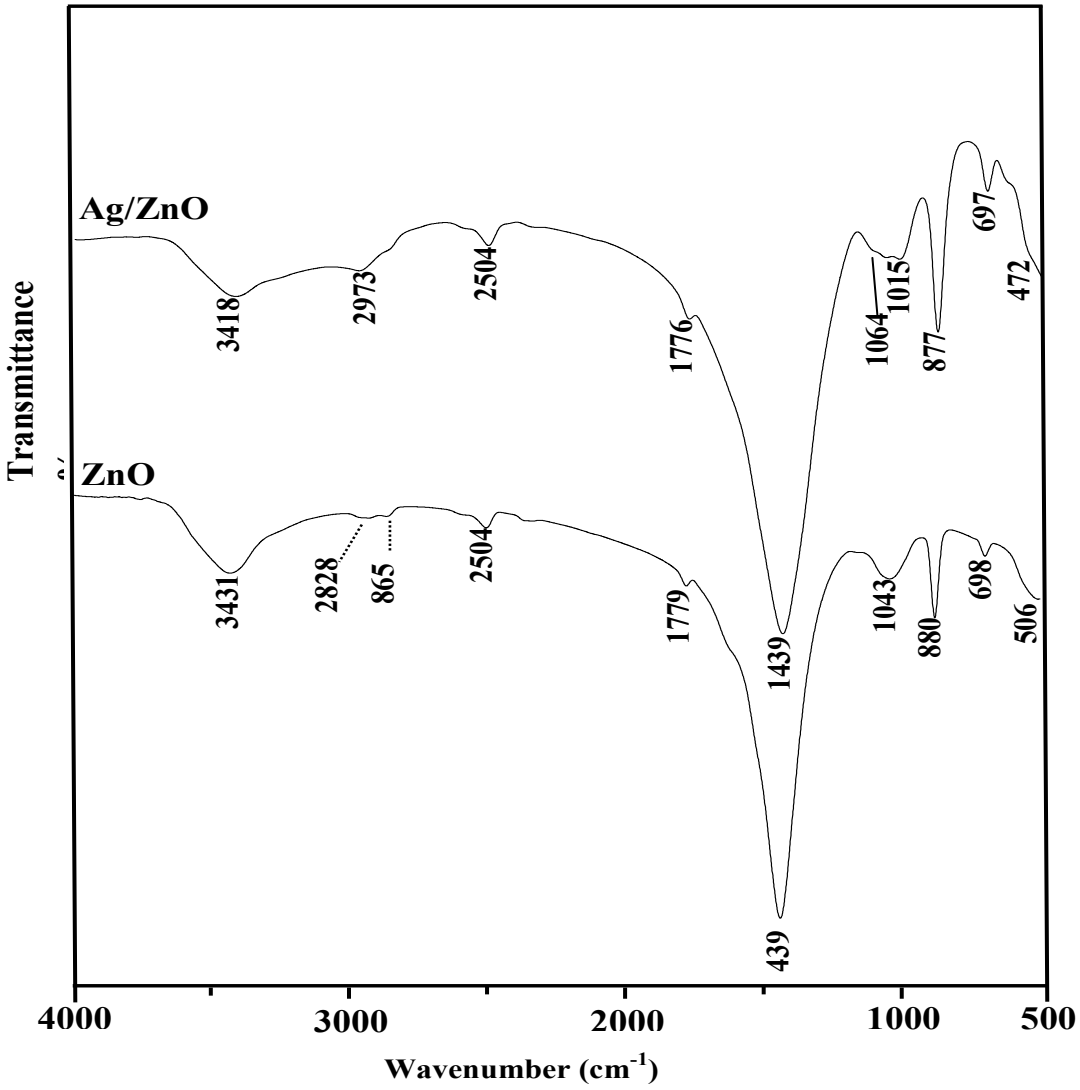

Fig. 2. IR spectra for synthetized zinc oxide nanoparticles and silver / zinc oxide nanocomposites.

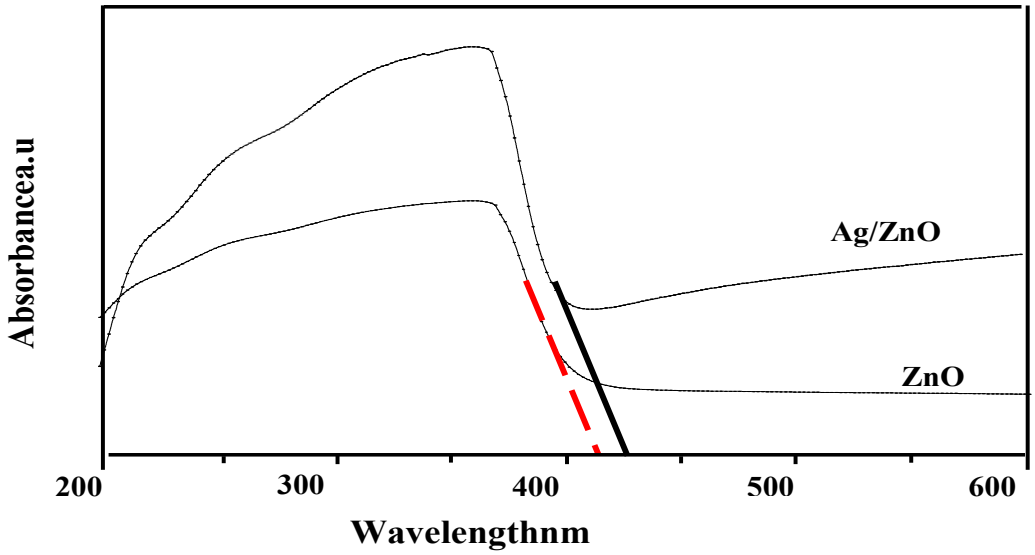

Fig. 3. UV-vis absorption spectra of zinc oxide nanoparticles and silver / zinc oxide nanocomposites.

The absorbance of the silver / zinc oxide composite increased even in visible light region and the absorption edge shifted towards higher wavelength with loading silver on zinc oxide, which is similar to findings of previous reports [41, 42]. Firstly, the red shift and enhanced absorptivity were due to the presence of crystalline Ag metal clusters in the nanoparticles and the incorporation of Silver ions (Ag^{+}) into the zinc oxide lattice sites.

SEM–EDX analysis

Surface morphology of the un-doped and silver-doped zinc oxide nanoparticles shown in Fig. 4. The SEM image of Zinc Oxide clearly show spherical-like shape in a dispersed and an agglomerated condition.

The SEM image of silver/zinc oxide particles remained spherical-like structure with increase-agglomerated particles and Silver nanoparticles were observed on the surfaces of zinc oxide microspheres, which suggests that the structure of zinc oxide was almost maintained after the formation of silver nano particles.

The elemental analysis of pure zinc oxide and silver / zinc oxide samples identified using EDX analysis as shown in Figure 5 and the chemical compositions of the elements identified in Table 1. EDX spectrum of zinc oxide shown peaks ascribed to Zn, O, and C elements observed and no peaks from other elements detected. The observed carbon peaks are due to the carbon remains on which the sample were preparing by CMC and absence of other elements reveal the purity of the nanomaterials. The presence of silver, zinc and oxygen peaks in silver / zinc oxide sample indicates that the successful dopants of silver into the zinc oxide.

AFM analysis

The AFM is a versatile and important tool to investigate the surface characteristics of synthesized samples. Figs. 5 and 6 show three-dimensional images of zinc oxide and silver/ zinc oxide samples with scanning area 5×5 µm. AFM images of zinc oxide observed a white spots large circular clusters involved in small spherical caps. These caps have a height in the range of 220 to 435 nm. AFM images related to doping silver on zinc oxide decreased the nanoparticle sizes with an average size of 70 to 155 nm and increased the surface roughness values.

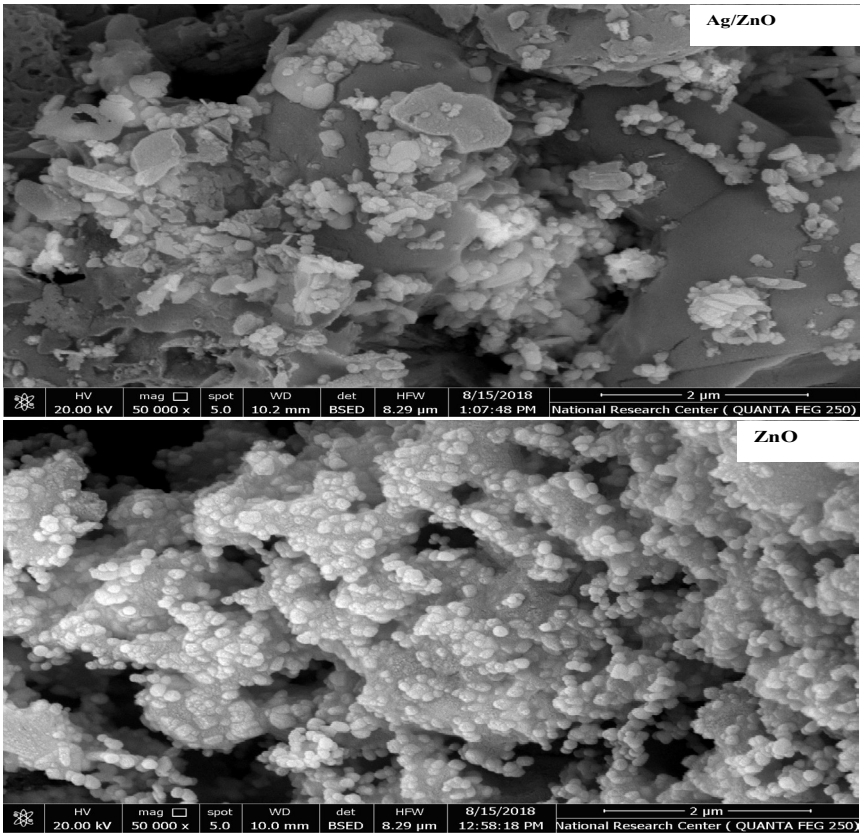

Fig. 4. The SEM image of zinc oxide nanoparticles and silver / zinc oxide nanocomposites.

TABLE 1. Elemental composition from EDX spectral analysis.

Samples	Elements									
	Na K		O K		Zn K		Ag L		C K	
	Wt. %	At. %	Wt. %	At. %	Wt. %	At. %	Wt. %	At. %	Wt. %	At. %
ZnO	24.74	25.8	18.63	27.92	40.97	15.03	--	--	15.66	31.26
Ag/ZnO	30.64	27.61	32.42	41.98	18.88	5.98	4.39	0.84	13.67	23.58

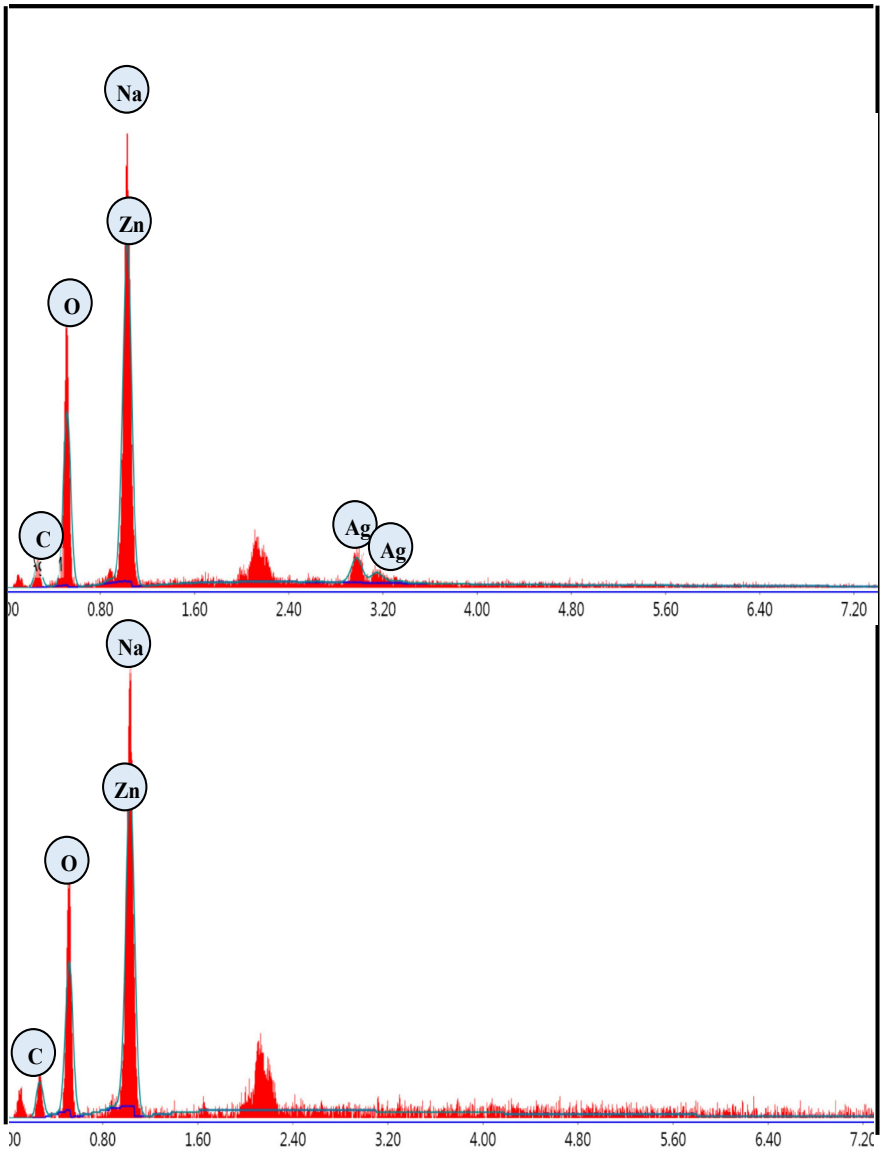

Fig. 5. EDX spectrum of zinc oxide nanoparticles and silver / zinc oxide.

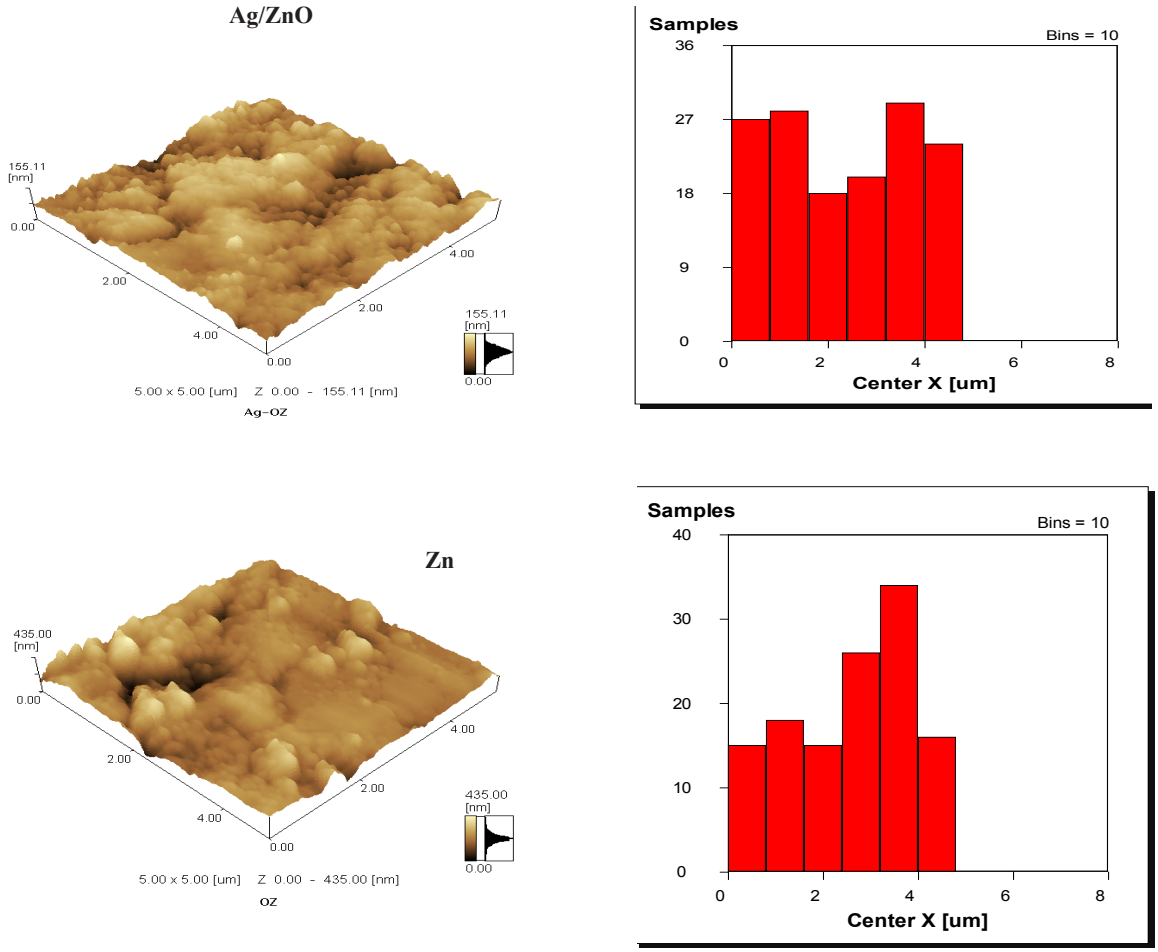

Fig. 6. AFM images of zinc oxide nanoparticles and silver / zinc oxide.

The SEM images of printed cotton fabrics using either silver / zinc oxide or zinc oxide nanoparticles (1 and 3% concentration) are shown in Fig. 7 and 8 respectively. From the results represent in Fig. 7 we noticed that, the surface of the printed cotton fabrics is uniformly and covered by the particles of zinc oxide nanoparticles, but in case of printed cotton with silver / zinc oxide nanoparticles (Fig. 8), we noticed that the surface of cotton is more homogeneity and silver / zinc oxide nano particles embedded on to the fabrics

Molecular modeling

The compatibility mixing of Carboxy methylcellulose with both ZnO and Ag was examined using Blends calculation in Materials Studio [43-45]. All calculated energies were summarized in (Table 2). This module was used to produce the final formulation of textile with optimized physical or chemical properties, at the lowest possible cost (Fig.9 A).

The mixing properties was discussed by Binding energy distribution, which obtained from Blends Mixing. (Fig. 9B) indicated that the distribution energy is almost similar for CMC-CMC (Ebb), CMC-ZnO (Ebb), and CMC-Ag (Ess), this is a good indicator that the structures will be compatible to mixing at 333 K. Furthermore, blending of CMC-ZnO is exhibited the higher interaction, mixing energy than CMC-Ag (Table 2), which indicted the distribution of ZnO through CMC more favorable than Ag.

MD simulation

Based on blinding energy simulated sample was choose for molecular dynamics simulation [46]. After the initial equilibration, MD production run was carried out for 10.0 ns. A series of snap shots taken at the regular time interval of 1.0 ns. Convergence and stability profiles for the MD simulation are interpreted in Fig. 10 A, B. RMSDs of MD structure have been plotted against time Fig. 10A.

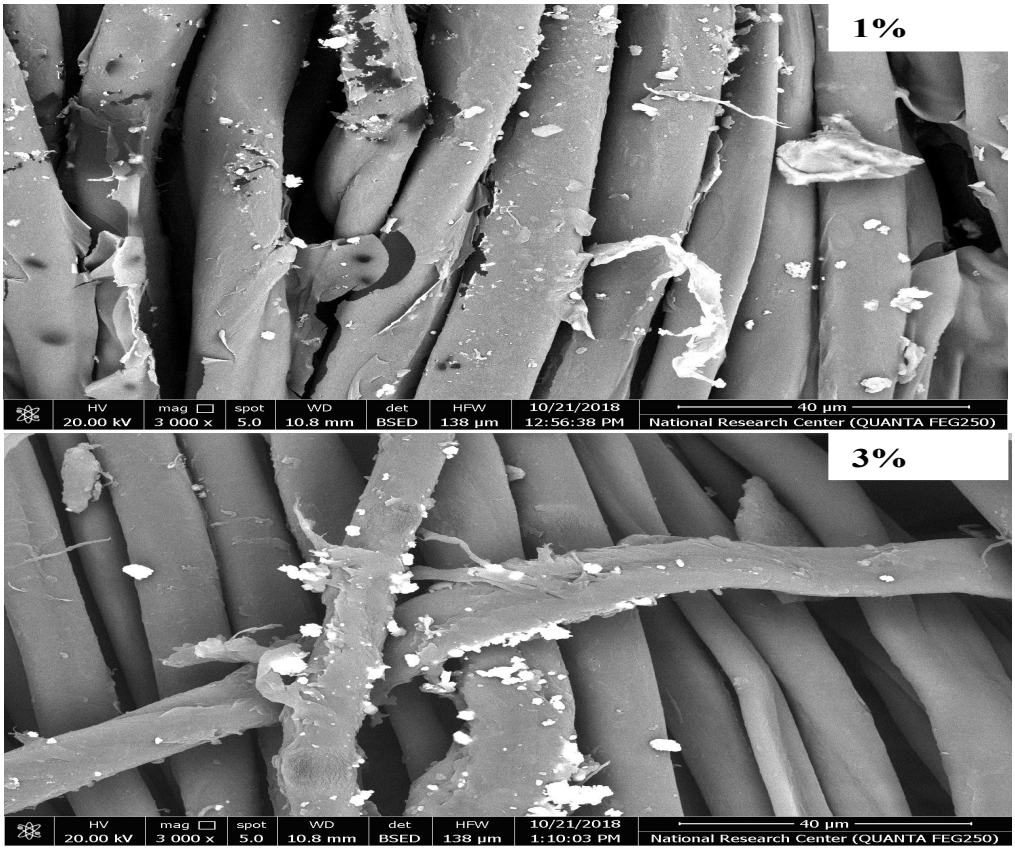

Fig. 7. SEM images of printed cotton fabrics using zinc oxide 1 and 3% concentration respectively.

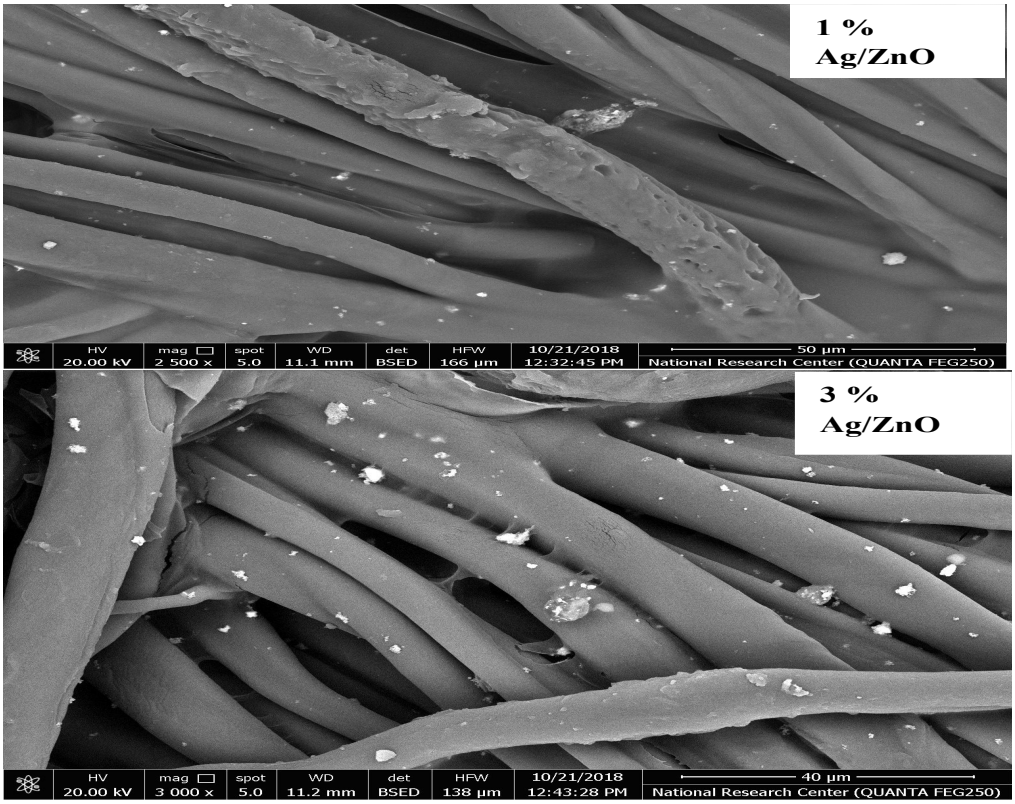

Fig. 8. SEM images of printed cotton fabrics using silver / zinc oxide 1 and 3% concentration respectively.

TABLE 2. Calculated energetic for synthesized sample at DFT with blending calculation using mixing Basics set.

Interacting energy	2.073898
total Mixing energy	1.228137
Mixing energy CMC-CMC	-0.94511
Mixing energy CMC-ZnO	-0.24056
Mixing energy CMC-Ag	-0.10164
Maximum distribution energy CMC-ZnO	-0.87342
Maximum distribution energy CMC-Ag	-0.35488
Maximum distribution energy CMC-CMC	-0.44463

A

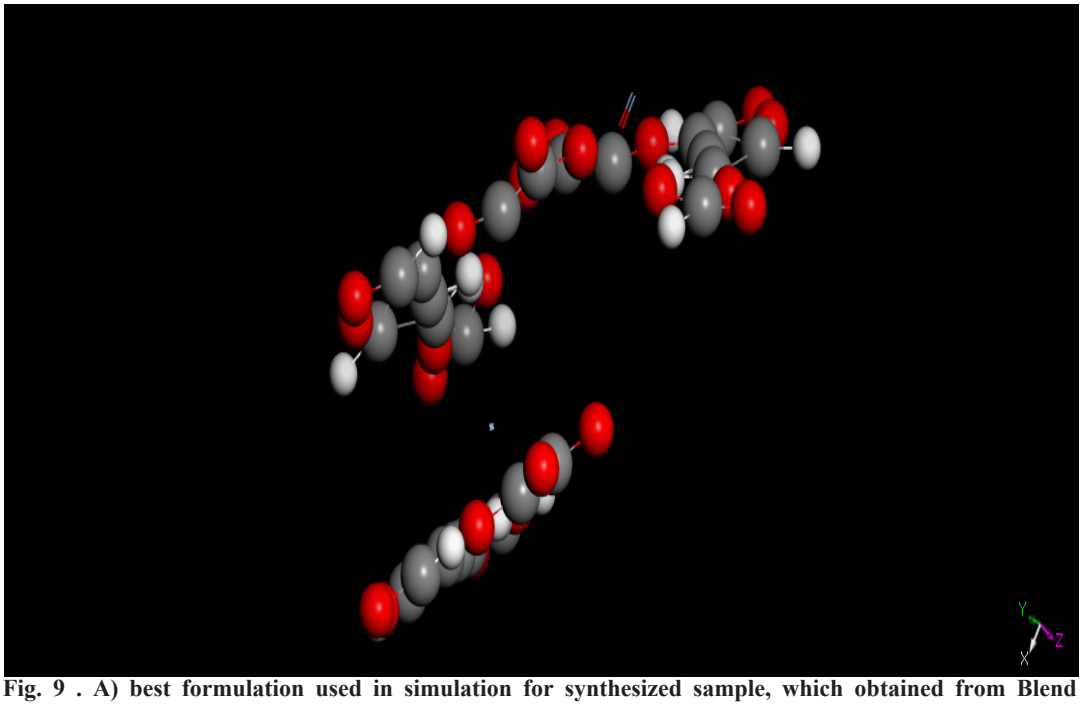

Fig. 9 . A) best formulation used in simulation for synthesized sample, which obtained from Blend calculation, CMC is represented as CPK mode and ZNO and Ag represented as line mode.

B

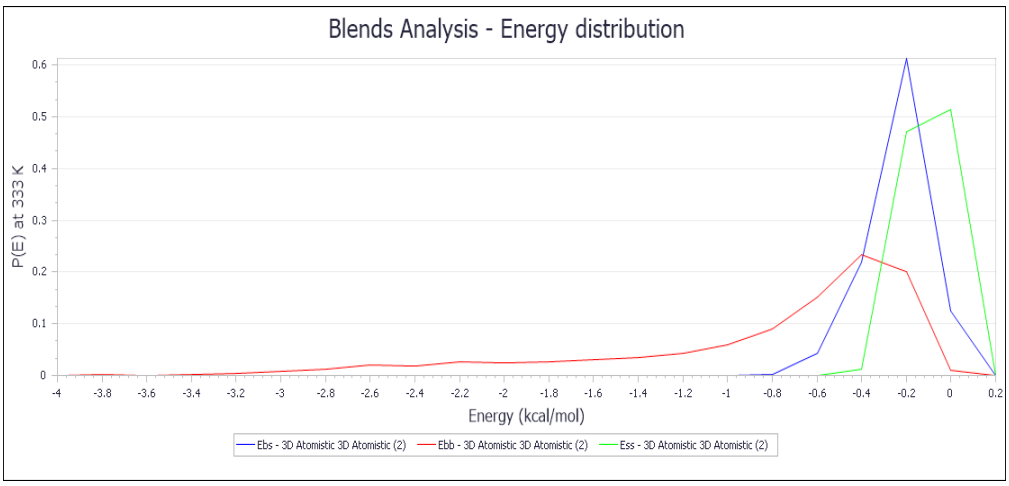

Fig. 9. B) Distribution of blending energy.

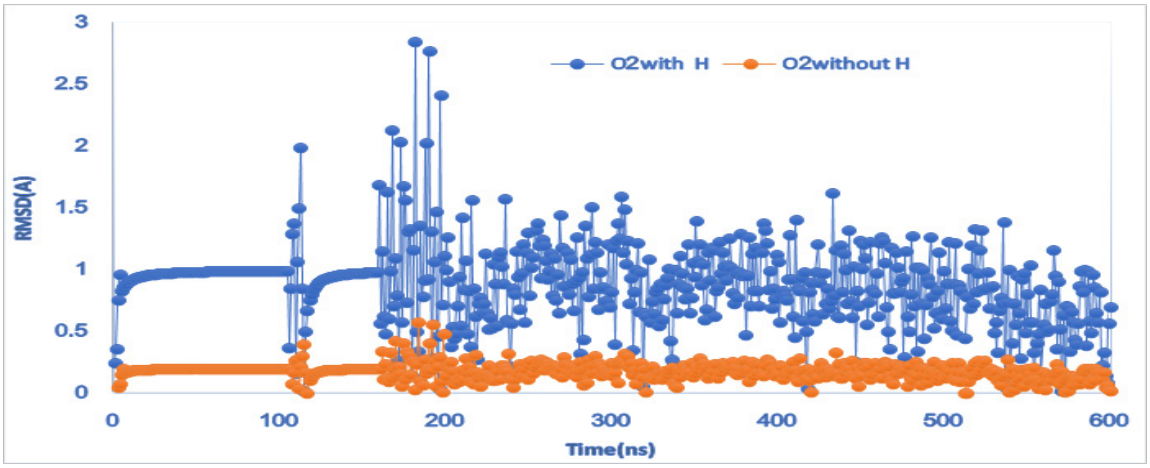

Fig. 10. Analysis of the MD simulation of synthesized sample. A) The snapshot of most stable sample during MD simulation at the interval of 1.0 ns.

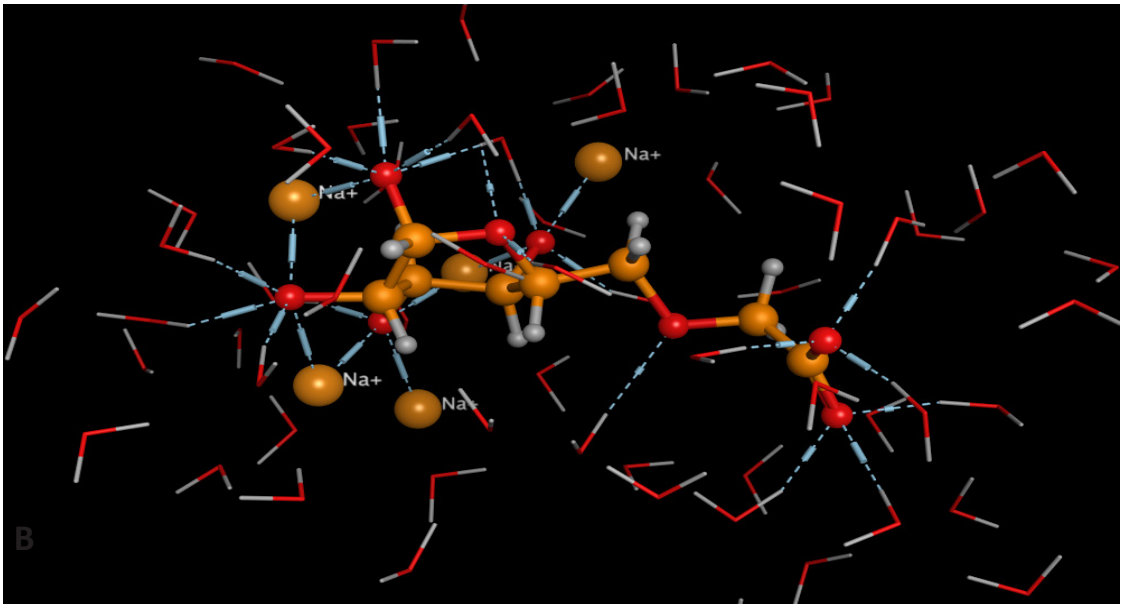

Fig. 10. B) Relationship between RMSD deviations of average MD simulated structure and function of time.

The results indicated that the MD structure shifted rapidly in the simulation to 3.1 Å RMSD from the initial structure, with reasonably small oscillations. The range of oscillation of the dynamical structure around the MD average is ±0.5 Å. The variation of total energy of the sample about (-0.6 to -13.5) kcal/mol (Table 3). It has been observed that the main contribution in the total energy comes out from the electrostatic energy and ionic energy is more negative than the hydrogen bond energy, which indicates about the good ability of sample to penetrate the cavity of water. RMSD calculations, energy variations for hydrogen and ionic interactions represented that the sample stability in solubility process.

TABLE 3. Key of interactions of the sample with water molecule derived from MD simulation.

Atom	Receptor		Interaction	Distance	E (kcal/mol)	Atom		Receptor	Interaction	Distance	E (kcal/mol)
O	1	HOH	H-acceptor	2.69	-3	O	19	HOH	H-acceptor	2.67	-2
O	1	HOH	H-acceptor	2.76	-2.9	O	24	HOH	H-acceptor	2.55	-2.9
O	1	HOH	H-acceptor	2.68	-2.9	O	24	HOH	H-acceptor	2.84	-1.2
O	1	HOH	H-acceptor	2.79	-2.8	O	24	HOH	H-acceptor	2.86	-1.1
O	6	HOH	H-acceptor	2.79	-1.9	O	24	HOH	H-acceptor	2.53	-2.2
O	6	HOH	H-acceptor	2.59	-5.7	O	24	HOH	H-acceptor	2.55	-2.5
O	6	HOH	H-acceptor	2.52	-4.4	O	24	HOH	H-acceptor	2.86	-1.2
O	6	HOH	H-acceptor	2.66	-6.1	O	24	HOH	H-acceptor	2.87	-0.8
O	6	HOH	H-acceptor	2.81	-1.6	O	24	HOH	H-acceptor	2.57	-2.9
O	6	HOH	H-acceptor	2.61	-5.9	O	25	HOH	H-acceptor	2.49	-1.5
O	6	HOH	H-acceptor	2.48	-3.6	O	25	HOH	H-acceptor	2.78	-2.8
O	6	HOH	H-acceptor	2.7	-6.1	O	25	HOH	H-acceptor	3.02	-2.7
O	8	HOH	H-acceptor	2.66	-6.2	O	25	HOH	H-acceptor	2.48	-1
O	8	HOH	H-acceptor	2.67	-6.3	O	25	HOH	H-acceptor	2.73	-2.8
O	8	HOH	H-acceptor	2.63	-6.4	O	25	HOH	H-acceptor	3.1	-2.4
O	8	HOH	H-acceptor	2.67	-6.6	O	6	NA	metal	2.22	-9.6
O	8	HOH	H-acceptor	2.67	-6.4	O	6	NA	metal	2.22	-9.6
O	8	HOH	H-acceptor	2.65	-5.9	O	8	NA	metal	2.2	-9.6
O	8	HOH	H-acceptor	2.6	-6.1	O	8	NA	metal	2.21	-9.5
O	8	HOH	H-acceptor	2.67	-6.1	O	10	NA	metal	2.16	-9.7
O	10	HOH	H-acceptor	2.63	-6.1	O	10	NA	metal	2.16	-9.7
O	10	HOH	H-acceptor	2.65	-5.8	O	11	NA	metal	2.2	-10.1
O	10	HOH	H-acceptor	2.6	-4.4	O	11	NA	metal	2.23	-10.1
O	10	HOH	H-acceptor	2.59	-5.8	O	6	NA	ionic	2.22	-12.4
O	10	HOH	H-acceptor	2.69	-5.8	O	6	NA	ionic	2.22	-12.4
O	10	HOH	H-acceptor	2.58	-4.1	O	8	NA	ionic	2.2	-12.8
O	11	HOH	H-acceptor	2.65	-6.4	O	8	NA	ionic	2.21	-12.6
O	11	HOH	H-acceptor	2.48	-4.1	O	10	NA	ionic	2.16	-13.4
O	11	HOH	H-acceptor	2.71	-5.5	O	10	NA	ionic	2.16	-13.5
O	11	HOH	H-acceptor	2.67	-5	O	11	NA	ionic	2.2	-12.8
O	11	HOH	H-acceptor	2.59	-6	O	11	NA	ionic	2.23	-12.4
O	11	HOH	H-acceptor	2.5	-4.7	Zn	1	HOH	metal	2.56	-1
O	11	HOH	H-acceptor	2.74	-5.1	Zn	1	HOH	metal	2.38	-1.3
O	11	HOH	H-acceptor	2.68	-5.1	Zn	1	HOH	metal	2.45	-0.6
O	19	HOH	H-acceptor	2.93	-0.9	Zn	1	HOH	metal	2.55	-1
O	19	HOH	H-acceptor	2.66	-2	Zn	1	HOH	metal	2.42	-1.2

Mobilities of nanoparticle molecules onto CMC molecules

Identification mobilities of nanoparticle is helpful to investigation of how water molecules affect diffusion behaviors for nanoparticle through CMC material [47]. The sample model was used for study ZnO mobilities through model which generated from blending calculation which mentioned above and were used to explore the mobilities (or RMSD) of nanoparticle molecules in adsorption sites. NPT MD simulation was preformed to identification of different types of driving forces, the H- and electrostatic interactions corresponding to adsorption site. Figure 10b exhibits variation of the RMSD value with time in the adsorption sites, which are in the presence and absence of water environment. In addition, in no water environment, nanoparticle molecule was found to have no apparent position variation in either H-bond system or ionic system. So, it can also be concluded that H-bond and electrostatic effect between nanoparticle and CMC should be the main driving forces to make nanoparticle molecules be adsorbed on the CMC and have slow-release properties in water or in water environment.

Antibacterial activity

The antibacterial activity was evaluated by measuring the clear zone inhibition around the test sample after 24 hr incubation. The effect of using either silver / zinc oxide and/or zinc oxide (1, 2, and 3 % concentration) for printing cotton fabrics, then drying the fabric at room temperature after that it was cured at 140°C for 3 min. on antimicrobial properties is shown in Table 4. It was found that printed cotton fabrics with both silver / zinc oxide nanoparticles 1, 2, and 3%, and/ or zinc oxide nanoparticles 3% have antibacterial activity but none of them has any antifungal activity on the tested microorganisms. The differences observed in the diameter of zone of inhibition between the printed cotton fabrics using silver / zinc oxide nanoparticles at different concentration and upon using zinc oxide, nanoparticles as shown in Fig. 11 may be due to the difference in the susceptibility of bacteria to the samples. Printed cotton fabrics with 3% silver / zinc oxide nanoparticles had the highest antibacterial activity; this is may be due to exhibited highest antioxidant effect. In addition, it was obviously clear that the tested samples are effective against Staphylococcus aureus (G+) growth higher than Escherichia coli (G-). This may be ascribed to

The thick layer around the cell wall of E. coli, which resists the penetration of antibacterial active material to their cell walls to interfere in its metabolic pathway.

It is evident that the silver / zinc oxide nanoparticles printed fabric showed higher antibacterial activity when compared with zinc oxide nanoparticles printed fabrics. The comparative antibacterial activity of silver / zinc oxide nanoparticles and zinc oxide nanoparticles, against Escherichia coli (G-) and Staphylococcus aureus (G+) were shown in Fig. 11 and Table 4.

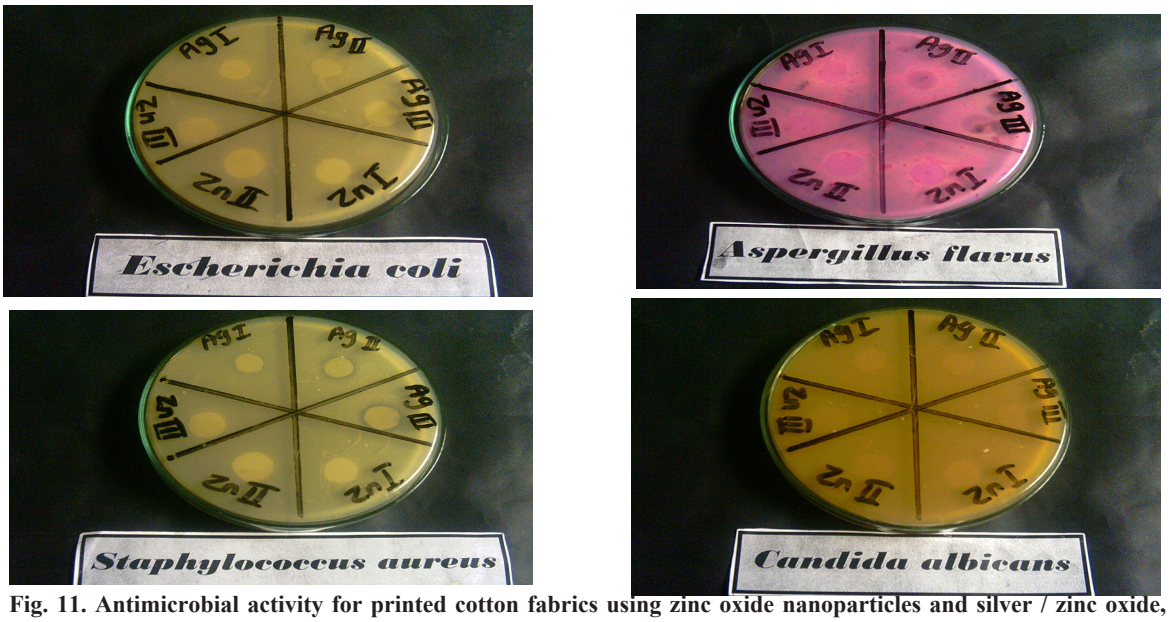

Fig. 11. Antimicrobial activity for printed cotton fabrics using zinc oxide nanoparticles and silver / zinc oxide, upon using 1 and 3% concentration.

TABLE 4. Effect of either Ag/ZnO or ZnO concentration on antimicrobial properties of finishing cotton fabrics.

Sample	(Inhibition zone diameter (mm / 1 cm Sample			
	Escherichia coli (G^-)	**Staphylococcus aureus (G^+)**	**Aspergillus flavus (Fungus)**	**Candida albicans (Fungus)**
Printed cotton fabrics with Ag/ZnO 1%	0.0	11	0.0	0.0
Printed cotton fabrics with Ag/ZnO 2%	11	12	0.0	0.0
Printed cotton fabrics with Ag/ZnO 3%	11	14	0.0	0.0
Printed cotton fabrics with ZnO **1%**	0.0	0.0	0.0	0.0
Printed cotton fabrics with ZnO **2%**	0.0	0.0	0.0	0.0
Printed cotton fabrics with ZnO **3%**	0.0	11	0.0	0.0

When assessed for antimicrobial activity by parallel streak method the printed fabric with silver / zinc oxide nanoparticles 3%, showed a maximum inhibitory effect against S. aureus with a zone of inhibition of 14 cm followed by E.coli with a zone of inhibition of 11 cm, but Printed cotton fabrics with zinc oxide 3% showed a maximum inhibitory effect against S. aureus with a zone of inhibition of 11 cm followed by *E.coli* with a zone of inhibition of 0 cm as shown in the Table 4.

Docking studies

The docking study have targeted DNA Gyrase to examine a mode of action of the small compounds as antimicrobial. The ligand–protein interaction behavior was estimated based on docking score function as implemented in MOE 2015.10 [48]. All calculations of docking experiment represented (Table 5). The crystal structures DNA gyrase (PDB: 4uro [49]) was obtained. The tested sample has been docked into active site of receptor. The ligands have been complexed with active site enzyme. The extracted docked poses of ligands were energy-minimized with molecular mechanics (MMFF94) force field, until the gradient convergence reached to 0.05 kcal/mol. The highest Molecular Operating Environment scoring function for tested compounds were applied to evaluate the binding affinities of tested compounds (Table 5).

The sample has been exhibited binding affinity with DNA gyrase (-3.794 Kcal/mol.). This sample combined with important amino acid residues (ARG84, ILE86, PRO 87, GLY125 and SER128) for DNA gyrase active site, which this formed a strong hydrogen bonds with short bond distances about (2.7- 3.07°) as shown in Fig. 12 and Table 6. The hydrophilicity of the Sample due to presence nanoparticles, which was the circular key for stabilizing the sample in receptor. The different interaction mode of sample with amino acids backbone in binding site (4uro) postulated that, the hydrophobicity and membrane permeability are an important pharmabiotic characters for absorption nanoparticle atoms of the sample in biological system. The results obtained clearly revealed that the amino acid residues close to the reference molecule is mostly the same as observed in all the tested compounds (Fig. 12 & 13).

TABLE 5 . Docking Energy scores (kcal/mol) derived frome the MOE for synthesized semple.

$E.d_{GE}$	$E_{\_conf}$	$E_{\_place}$	$E._{Int}$	E_{ele}	$\_r_{msd}$
-3.79708	-490.984	-70.0817	-15.685	-20.9747	0.953509

$E_{\_score1;}$ Initial free binding energy of the ligand from a given pose. $E_{d.G.}$: Final free binding energy of the ligand from a given pose, $E_{\_conf;}$ Free binding energy of the ligand from a given conformer. $E_{\_place.}$ Free binding energy of the ligand from a receptor. $E._{Int.}$**:** Affinity binding energy of ligand with receptor, Eele: Electrostatic interaction with the receptor. ***RMSD***; The root mean square deviation of the pose of the docking pose compared to the co-crystal ligand position.

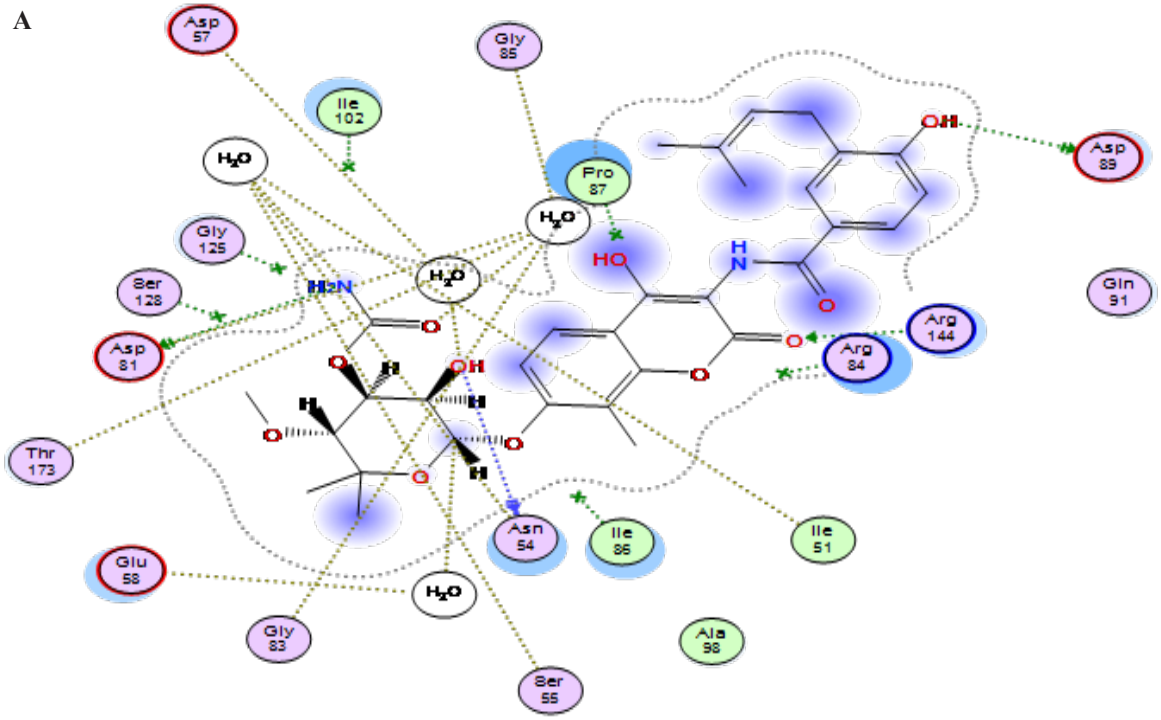

Fig. 12. The tested sample was docked into the active site of DNA gyrase using MOE tool, A) 2D interaction mode,

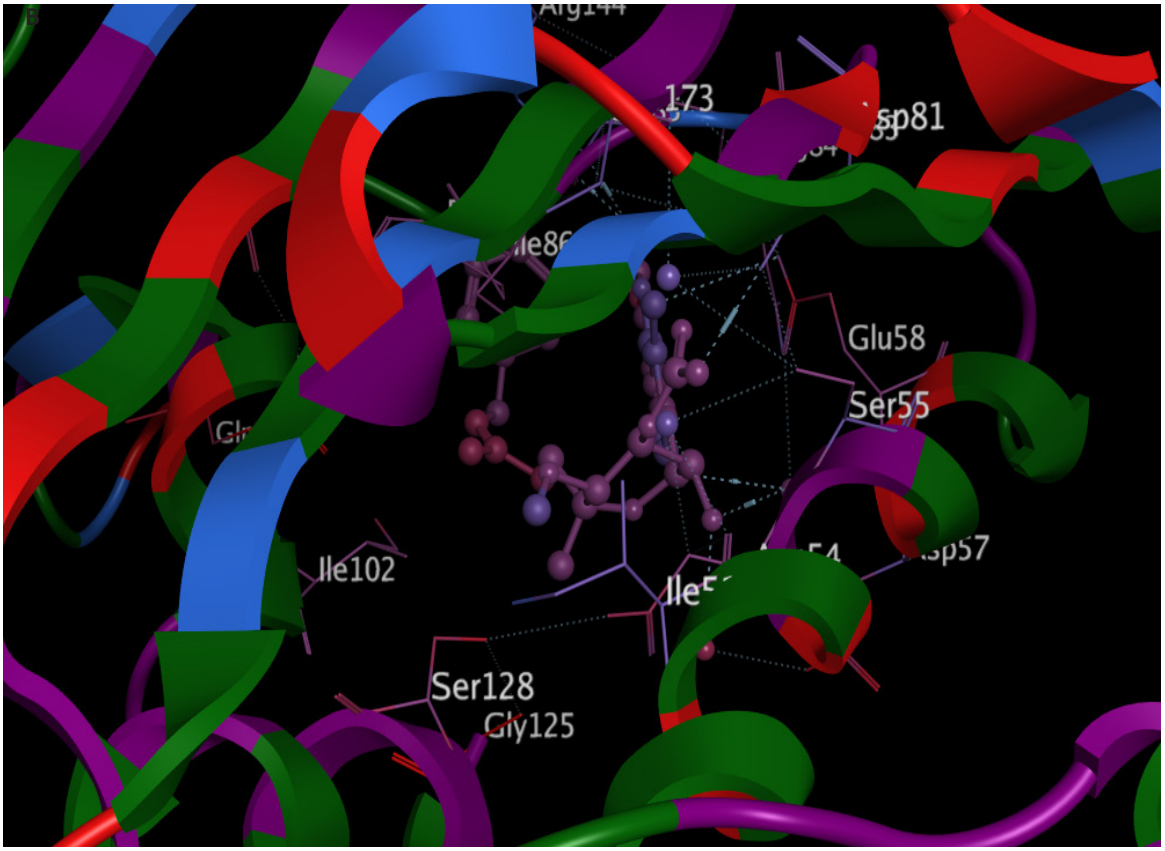

Fig. 12. B) 3D interaction mode, H- bonds are in blue.

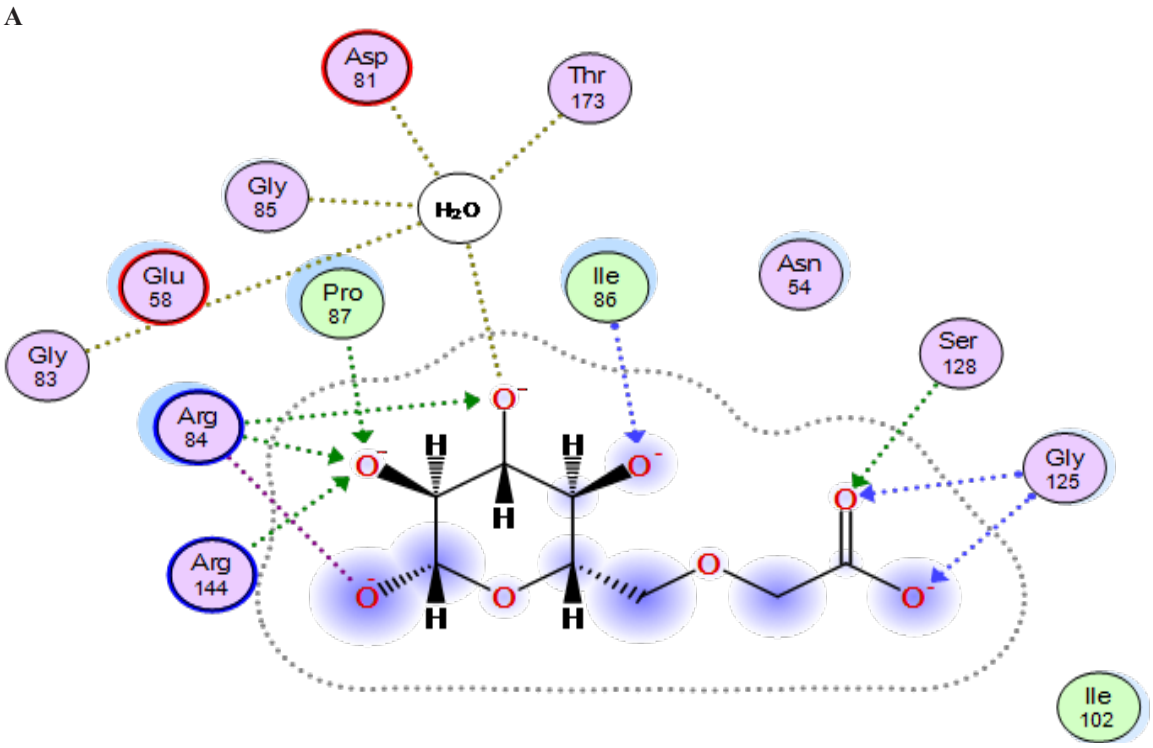

Fig. 13. The reference inhibitor was docked into the active site of DNA gyrase using MOE tool, A) 2D interaction mode.

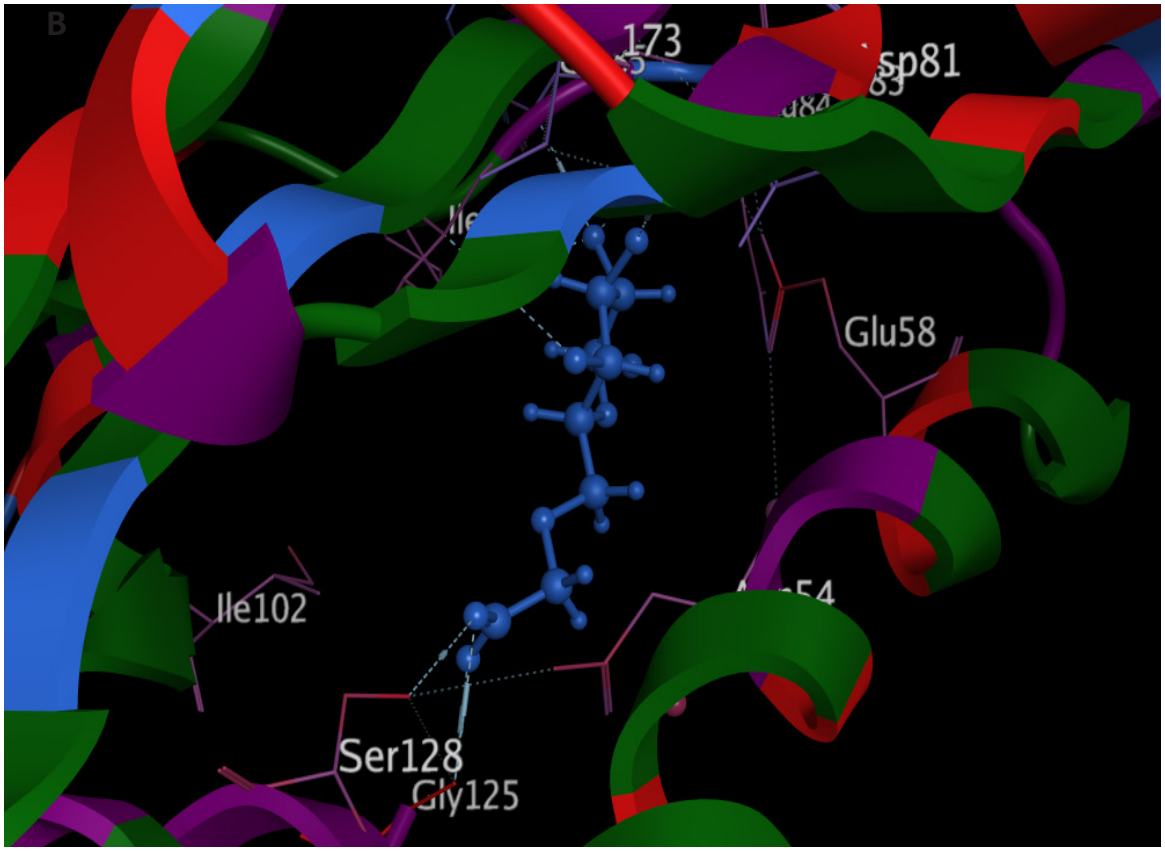

Fig. 13. B) 3D interaction mode, H- bonds are in blue.

TABLE 6. Key of interactions of the newly synthesized sample with active site.

Atom		Receptor				Interaction	Distance	E(kcal/mol)
O	6	CA	ILE	86	(A)	H-acceptor	2.72	-0.8
O	8	CB	ARG	84	(A)	H-acceptor	2.51	-1.3
O	8	O	HOH	2013	(A)	H-acceptor	2.28	-4.4
O	11	CB	ARG	84	(A)	H-acceptor	2.41	-1.7
O	11	CD	PRO	87	(A)	H-acceptor	2.72	-0.8
O	11	NH1	ARG	144	(A)	H-acceptor	2.88	-11.2
O	24	N	GLY	125	(A)	H-acceptor	2.07	-9.4
O	24	OG	SER	128	(A)	H-acceptor	2.4	-0.9
O	25	N	GLY	125	(A)	H-acceptor	2.07	-6
O	10	NE	ARG	84	(A)	ionic	2.84	-0.8
O	10	NH1	ARG	84	(A)	ionic	2.78	-1
O	10	NH2	ARG	84	(A)	ionic	2.3	-2.7
O	11	NE	ARG	84	(A)	ionic	2.65	-1.4
O	11	NH1	ARG	144	(A)	ionic	2.88	-5.4
O	24	N	GLY	125	(A)	ionic	3.07	-4
O	25	N	GLY	125	(A)	ionic	3.07	-4

Conclusion

The results show that, silver / zinc oxide nanoparticles printed fabric showed the highest antibacterial activity when compared with zinc oxide nanoparticles printed fabrics, and higher antibacterial activity was observed against S. aureus than E. coli. A simple method had been developed to prepare silver / zinc oxide and zinc oxide nanoparticles. Printed cotton fabrics with both silver / zinc oxide nanoparticles 1, 2, and 3%, and zinc oxide nanoparticles 3% have antibacterial activity against, Staphylococcus aureus and Escherichia coli, *i.e.* medical textile. Blends mixing calculation indicted the distribution of ZnO through CMC more favorable than Ag. Blends mixing calculation indicted the distribution of ZnO through CMC more favorable than Ag. Molecular dynamic calculation demonstrated that H-bond and electrostatic effect between nanoparticle and CMC should be the main driving forces to make nanoparticle molecules be adsorbed on the CMC and have slow-release properties in water or in water environment.

The SEM analysis of the silver / zinc oxide nanoparticles printed cotton fabric found that, the surface of cotton is more homogeneity and silver /zinc oxide nano particles embedded on to the fabrics.

Acknowledgements

The authors of this article gratefully acknowledge the Jouf University, Sakaka, Saudi Arabia, for financially support this work (project number 96/39).

Reference

1. Rajendran R, Balakumar C, Ahammed HAM, Jayakumar S, Vaideki K, Rajesh EM. Use of zinc oxide nano particles for production of antimicrobial textiles. *Inter. J. Eng. Sci. Techn*. **2**: 202-208 (2010).

2. Hossam E. Emam. Generic strategies for functionalization of cellulosic textiles with metal salts. *Cellulose* **26**:1431–1447. (2019)

3. El-Nahhal IM, Zourab SM, Kodeh FS, Elmanama AA, Selmane M, Genois I, Babonneau F. Nano-structured zinc oxide–cotton fibers: synthesis, characterization and applications. *J. Mater. Sci. Mater. Electronics,* 24: 3970-3975 (2013).

4. El-Nahhal IM, Zourab SM, Kodeh FS, Selmane M, Genois I, Babonneau F .Nanostructured Copper Oxide-Cotton Fibers: Synthesis, Characterization, and Applications. *Intern. Nano Letters,* **2**: 1-5(2012).

5. Firdhouse MJ, Lalitha .Corrosion Inhibition of Mild Steel in Acidic Media by 5′-Phenyl-2′, 4′-dihydrospiro [indole-3, 3′-pyrazol]-2 (1H)-one. *J. Chemistry,* 2013:1-9 P (2013).

6. Abramova A, Gedanken A, Popov V, Ooi EH, Mason TJ, Joyce EM, Beddow J, Perelshtein I, Bayazitov V.A sonochemical technology for coating of textiles with antibacterial nanoparticles and equipment for its implementation. *Mater. Letters,* 96: 121-124, (2013).

7. I. Perelshtein, A. Lipovsky, N. Perkas, A. Gedanken, E Moschini, P. Mantecca .The influence of the crystalline nature of nano-metal oxides on their antibacterial and toxicity properties. *Nano Research.* 8: 695-707 (2015).

8. Manna A C .Synthesis, characterization, and antimicrobial activity of zinc oxide nanoparticles. Nano-Antimicrobials. *Bio Nano Sci.* 2:329–335 (2012).

9. Chan CMN, Cheng HS, Djurisic AB, Ng AMC, Leung FCC, Chan WK .Multicomponent antimicrobial transparent polymer coatings*, J. Appl. Polym. Sci.*122:1572-1578(2011).

10. Gokulakrishnan R, Ravi Kumar S, Raj JA. In vitro antibacterial potential of metal oxide nanoparticles against antibiotic resistant bacterial pathogens. *Asian Pac. J. Trop. Dis.* 2: 411-413(2012).

11. Rai M, Yadav A, Gade A .Silver nanoparticles as a new generation of antimicrobials*. Biotechnol. Adv.* 27: 76-83(2009).

12. da Silva FAG, Queiroz JC, Macedo ER, Fernandes AWC, Freire NB, da Costa MM, de Oliveira HP .Antibacterial behavior of polypyrrole: The influence of morphology and additives incorporation, Mater. Sci. Eng. C, Mater. *Biol. Appl.* 62: 317–322(2016).

13. Eren O, Ucar N, Onen A, Kizildag N, Karacan I .Synergistic effect of polyaniline, nano silver, and carbon nanotube mixtures on the structure and properties of poly acrylonitrile composite nanofiber. *J. Compos. Mater.* 50: 2073-2086 (2016).

14. Youssef AM, Mohamed SA, Abdel-Aziz MS, Abdel-Aziz ME, Turky G, Kamel S .Biological studies and electrical conductivity of paper sheet based on polyaniline/ PS/Ag NPs nanocomposite. *Carbohydrate Polym.* 147:333–343 (2016).

15. Stejskal J .Conducting polymer–silver composites. *Chem. Pap.* 67: 814–848 (2013).

16. Alekseeva E, Bober P, Trchová M, Šed nková I, Prokeš J, Stejskal J .The composites of silver with globular or nano tubular poly pyrrole: The control of silver content. *Synth. Met.* 209:105–111(2015).

17. Wan CC, Li J. Cellulose aerogels functionalized with poly pyrrole and silver nanoparticles: In-situ synthesis, characterization and antibacterial activity. *Carbohydrate Polym.* 146: 362–367(2016).

18. Mu SP, Xie HY, Wang W, Yu D .Electroless silver plating in PET fabric initiated by in situ reduction of polyaniline. *Appl. Surf. Sci.* 353: 608–614(2015).

19. Škodová J, Kopecký D, Vr ata M, Varga M, Prokeš J, Cieslar M, Bober P, Stejskal J .Poly pyrrole–silver composites prepared by the reduction of silver ions with poly pyrrole nanotubes. *Polym. Chem.* 4: 3610–3616(2013).

20. Tiam J, Wong KKY, Ho CM, Lok CN, Yu W-Y, Che C-M, Chiu J-F, Tam PKH .Topical delivery of silver nanoparticles promotes wound healing. *Chem Med Chem.* 2: 129-136 (2007).

21. Reznickova A, Slavikova N, Kolska Z, Kolarova K, Belinova T, Kalbacov MH, Cieslare M, Svorcika V .PEGylated gold nanoparticles: Stability, cytotoxicity and antibacterial activity. *Colloids and Surfaces A:* 560:26-34 (2019).

22. Cady NC, Behnke JL, Strickland AD .Copper Based Nanostructured Coatings on Natural Cellulose: Nanocomposites Exhibiting Rapid and Efficient Inhibition of a Multi Drug Resistant Wound Pathogen, A. baumannii, and Mammalian Cell Biocompatibility In Vitro. Adv. *Funct. Mater.* 21:2506–2514 (2011).

23. O. Akhavan, E. Ghaderi .Cu and CuO nanoparticles immobilized by silica thin films as antibacterial materials and photo catalysts. *Surf. Coat. Technol.,* 205, 219-223 (2010).

24. Kong H, Song J, Jang J .Photo catalytic. *Environ. Sci. Technol.* 2010, 44: 5672–5676 (2010).

25. Nithyaa K, Kalyanasundharam S .Effect of chemically synthesis compared to biosynthesized ZnO nanoparticles using aqueous extract of C. halicacabumand their antibacterial activity. *Open Nano* 4:100024 (2019).

26. Morfesis A, Fairhurst D. at NSTI Nanotechnology Conference and Trade Show. NSTI Nanotech Anaheim, CA May 8-12 (2005).

27. Karunakaran C, Gomathisankar P, Manikandan G .Preparation and characterization of antimicrobial Ce-doped ZnO nanoparticles for photocatalytic detoxification of cyanide. *Mater. Chem. Phys*.123:585-594 (2010).

28. Salama TM, Ali IO, Gumaa HA, Lateef MA, Bakr MF .Novel synthesis of nay zeolite from rice husk silica: modification with ZnO and ZnS for antibacterial application. *Chem. Sci J,* 7: 1-9 (2016).

29. Li LH, Deng JC, Deng HR, Liu ZL, Li XL .Preparation, characterization and antimicrobial activities of chitosan/ Ag/ZnO blend films. *Chem. Eng. J.,* 160, 378-382 (2010).

30. Lu WW, Liu GS, Gao SY, Xing ST, Wang JJ .Tyrosine-assisted preparation of Ag/ZnO nanocomposites with enhanced photocatalytic performance and synergistic antibacterial activities. *Nanotechnology,* 19:doi: 10.1088/0957-4484/19/44/445711(2008).

31. Manna J, Goswami S, Shilpa N, Sahu N, Rana RK .Biomimetic Method to Assemble Nanostructured Ag/ZnO on Cotton Fabrics: Application as Self-Cleaning Flexible Materials with Visible-Light Photo catalysis and Antibacterial Activities Appl. Mater. *Interfaces.* 7: 8076–8082 (2015).

32. Marzieh Khademalrasoo, Mansoor Farbod, and Azam Iraji zad. Preparation of ZnO nanoparticles/ Ag nanowires nan composites as plasmonic photo catalysts and investigation of the effect of concentration and diameter size of Ag nanowires on their photo catalytic performance. *Journal of Alloys and Compounds* Volume 664, 15 April, Pages 707-714 (2016)

33. Ibraheem Othman Ali. Synthesis and characterization of Ag0/PVA nanoparticles via photo- and chemical reduction methods for antibacterial study. *Colloids and Surfaces A: Physicochemical and Engineering Aspects* Volume 436, 5 September, Pages 922-929 (2013)

34. Zheng Y, Chen C, Zhan Y, Lin X, Zheng Q, Wei K, Zhu J .Photo catalytic. *J. Phys. Chem.* 112: 10773-10777 (2008).

35. Yamamoto T, Katayama-Yoshida H .Solution using a codoping method to unipolarity for the fabrication of p-type ZnO. *Jpn. J. ppl. Phys.* 38: L166 (1999).

36. Wahab R, Ansari SG, Kim YS, Seo HK, Kim GS, Khang G, Shin H-S .Low temperature solution synthesis and characterization of ZnO nano-flowers. *Materials Research Bulletin,* 42:1640–1648 (2007).

37. T. K. Gupta, P. L. Hower .A comparative study of Si and GaAs based devices for repetitive, high energy, pulsed switching applications. *J. App. Phys.* 50: 4847 (1992).

38. Parvin T, Keerthiraj N, Ibrahim IA, Phanichphant S, Byrappa K .Photocatalytic Degradation of Municipal Wastewater and Brilliant Blue Dye Using Hydrothermally Synthesized Surface-Modified Silver-Doped ZnO Designer Particles. *Inter. J. of Photo Energy,* 67:610-618 (2012).

39. Karami H, Fakoori E .Synthesis and Characterization of ZnO Nano rods based on a New Gel Pyrolysis Method. *J. of Nano mater, doi:10.1155/2011/628203(2011).*

40. Ni Y, Cao X, Wu G, Hu G, Yang Z, Wei X .Preparation, characterization and property study of zinc oxide nanoparticles via a simple solution-combusting method. *Nanotech.* 18:155603 (2007).

41. Lee E, Hong J, Kang H, Jang J .Synthesis of TiO2 nano rod-decorated graphene sheets and their highly efficient photo catalytic activities under visible-light irradiation. *J. Hazard. Mater.* 219–220: 13-18 (2012).

42. Height MJ, Pratsinis SE, Mekasuwandumrong O, Praserthdam P, .Ag-ZnO catalysts for UV-photo degradation of methylene blue, *Appl. Catal. B. 63 : 305-312(2006).*

43. Nemirovsky, A. M.; Bawendi, M. G.; Freed, K. F. J, Lattice models of polymer solutions: Monomers occupying several lattice sites. *Chem. Phys.,* 87, 7272(1987).

44. Pesci, A. I.; Freed, K. F. J., .Lattice models of polymer fluids: Monomers occupying several lattice sites. II. Interaction energies. *Chem. Phys.,* 90, 2003 (1989).

45. Schweizer, K. S.; Curro, J. G. J., .Integral equation theory of the structure and thermodynamics of polymer blends. *Chem. Phys.*, 91, 5059 (1989).

46. Vu T., Chaffee A., and Yarovsky I. Investigation of lignin – water interactions by molecular simulation. *Mol. Simul.* 28, 981 – 991 (2002).

47.Derreumaux P, Schlick TJPS, Function, Bioinformatics. Long timestep dynamics of peptides by the dynamics driver. *Approach*. 21(4):282-302 (1995)

48. Molecular Operating Environment (MOE) CCGU, 1010 handbook St. West, Suite 910, Montreal, QC, Canada, H3A 2R7. (2017).

49. Dale, Glenn E., et al. "Crystal engineering: deletion mutagenesis of the 24 kDa fragment of the DNA gyrase B .Subunit from Staphylococcus aureus." Acta Crystallographica Section D: *Biological Crystallography,* 55.9: 1626-1629 (1999).

تحضير أكسيد الزنك وأكسيد الزنك مع الفضة Nano composite لإنتاج المنسوجات المضادة للبكتيريا

ابراهيم عثمان على ابوزيد [٢،١] و محمد مبروك محمد الملا [٣،١]

[١]قسم الكيمياء -كلية العلوم والآداب بالقريات -جامعة الجوف -المملكة العربية السعودية

[٢]قسم الكيمياء – كليه العلوم جامعة الازهر – مدينه نصر –القاهرة -مصر

[٣]قسم الصباغة والطباعة – شعبه بحوث الصناعات النسيجية، المركز القومي للبحوث، شارع البحوث، الدقي، الجيزة، مصر.

تم تحضير جسيمات من أكسيد الزنك النانوية وكذلك تخليق الجسيمات النانوية أكسيد الزنك مع الفضة بتفاعل نترات الفضة مع أكسيد الزنك في خطوة واحدة، تم طباعه هذه المركبات على اقمشه القطن بنسبة ١٠٠٪ باستخدام معجون الطباعة التي تحتوي على هذه المركبات. وتم تثبيت هذه المركبات على الأقمشة القطنية بواسطة التجفيف عند درجة حرارة منخفضة ثم التثبيت الحراري. تم اثبات التفاعل الكيميائي لأكسيد الزنك وأكسيد الزنك مع الفضة باستخدام تقنيات مختلفة مثل الأشعة السينية X ray وتحليلات AFM، أطياف الأشعة تحت الحمراء، المجهر الإلكتروني المسح الضوئي (SEM) ..... إلخ.

تم تقييم النشاط المضاد للبكتيريا للأقمشة القطنية المطبوعة بأكسيد الزنك أو أكسيد الزنك مع الفضة ضد، المكورات العنقودية الذهبية وإيشيريشيا كولي وقد أجريت دراسة للإشارة إلى سلوك التفاعل مع الحمض النووي في الكائنات الحية الدقيقة. وأظهرت هذه الدراسة أن بسبب وجود الجسيمات النانوية والتي كانت المفتاح لتثبيط الكائنات الحية الدقيقة. نشأت حداثة هذا العمل من قدرته على تلبية متطلبات الجدوى الاقتصادية للمنسوجات الطبية.